Available online at www.sciencedirect.com
SCIENCE DIRECT®
Chemical Physics Letters 372 (2003) 73–81
CHEMICAL PHYSICS LETTERS
www.elsevier.com/locate/cplett

The effect of excitation pulse carrier frequency on ultrafast charge recombination dynamics of excited donor–acceptor complexes

A.I. Ivanov [a,*], F.N. Belikeev [a], R.G. Fedunov [a], E. Vauthey [b]

[a] *Department of Physics, Volgograd State University, 2-nd Prodolnaya Str., 30, Volgograd, 400062, Russia*
[b] *Department of Physical Chemistry, University of Geneva, 30 quai Ernest Ansermet, CH-1211 Geneva, Switzerland*

Received 15 January 2003

Abstract

The excitation of a charge transfer band by a laser pulse of finite duration and the ensuing charge recombination are calculated in the framework of the perturbation theory. The influence of the spectral characteristics of the laser pulse on the charge recombination dynamics is investigated for models including several nuclear modes that differ greatly in their timescales. It is shown that, in the area of applicability of the perturbation theory, the variation of the pulse carrier frequency inside the absorption band can significantly change the effective charge recombination rate constant.

1. Introduction

The time resolution of modern femtosecond laser spectroscopy allows the real-time investigation of the dynamics of electron transfer (ET) reactions, which are substantially faster than solvent relaxation [1–12]. The typical oscillations reflecting coherent wave-packet motion have been also observed in ET reactions dynamics [5,7,8]. These features of ultrafast ET undoubtedly point out on the conservation of the memory on the initial vibrational state in such processes. This implies that the preparation of the initial electronic state from which ET occurs is of primary importance and therefore should be carefully described in any theoretical approach pretending to a quantitative description of the phenomenon.

The initial state is usually populated by a short laser pulse and in this case, the preparation process can be quantitatively described. Moreover, the photoexcitation and the following ultrafast back ET should be considered as a joint process, because for pulse duration of hundred and even tens femtoseconds there is an overlapping between excitation and reverse charge transfer dynamics [9].

Theoretical studies of the role of the non-equilibrium initial conditions in electronic transitions dynamics have been carried out for nearly 40 years. Theories were first developed to describe the time-dependent fluorescence [13–19]. Recently different aspects of non-equilibrium effects in ultrafast ET dynamics were investigated [20–26].

* Corresponding author. Fax: +7-8442-433786.
E-mail address: ivanov@physic.wgu.tsaritsyn.su (A.I. Ivanov).

0009-2614/03/$ - see front matter
doi:10.1016/S0009-2614(03)00363-4

An expression for the population decay from an initially prepared electronic state with a non-equilibrium nuclear distribution to a second non-adiabatically coupled electronic state was derived and called the non-equilibrium golden rule formula [22]. For photoinduced ET, the importance of optical preparation of a non-equilibrium nuclear distribution in the donor state was shown in the limit of ultrashort pulse (delta-function) [23]. This problem had to be considered in the framework of the three-state model, with an additional state optically coupled to the donor state. Excitation effects on the quantum dynamics of two-dimensional photoinduced non-adiabatic processes have been numerically explored in reference [25]. The Franck–Condon activity in the various vibrational modes was shown to have a significant effect on the electron transfer probability when motion in the reactant well is underdamped.

In this Letter, we investigate the ET dynamics in donor–acceptor complexes. These complexes are characterized by a broad absorption band in the UV–vis due to a charge transfer transition. Excitation in this band leads to an excited state, which can be considered as a contact ion pair. The major reaction pathway of this excited state is the non-radiative transition to the ground state, corresponding to a charge recombination (CR) process. The goals of this report is to evaluate the effect of carrier frequency and duration of the excitation pulse on the CR dynamics in polar solvents and to relate this dependence on parameters specific to the donor–acceptor complex and to the medium.

2. Evaluation of time-dependent populations and rates

We consider the photoexcitation of a donor–acceptor complex in polar solvent to a charge separated state and the ensuing CR. The idea of the influence of the carrier frequency on the CR dynamics can be demonstrated on a single reaction coordinate model (Fig. 1). The higher the excitation frequency, the further from the term crossing point the wave-packet is placed. Therefore, the time required to reach the term crossing point

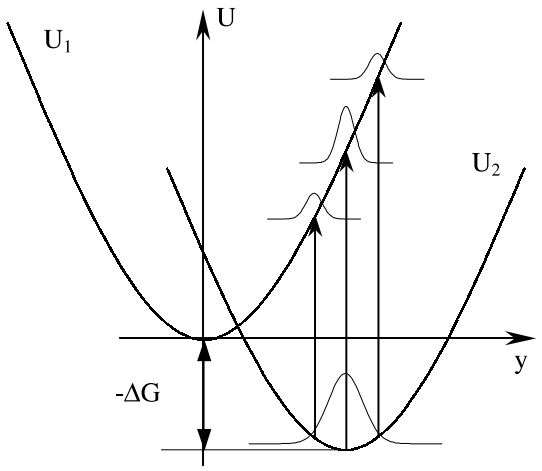

Fig. 1. Diabatic free energy curves displaying the ground and excited electronic states. The initial wave-packet corresponds to the equilibrium distribution in the ground state. The arrows represent the optical excitation of the system. The initial position of the wave-packet in the excited state depends on the pulse carrier frequency. The length of the arrows is proportional to the excitation frequency.

where CR occurs increases with frequency. This results in a decrease of the effective rate constant. For non-adiabatic reactions, the vast majority of the transitions takes place after the wave-packet has passed through the term crossing point. As a consequence, the effect of a variation of the excitation frequency can be expected, at first glance, to be insignificant. Nevertheless, this effect can be fairly large when two or more reaction coordinates with greatly different relaxation times are involved.

To describe the photoexcitation and the following CR, the so-called two-level approximation is used. The Hamiltonian of the system can be written in the form

$$\begin{pmatrix} H_1 & \widetilde{V}(t) \\ \widetilde{V}^*(t) & H_2 \end{pmatrix}, \tag{1}$$

where

$$H_1 = \frac{1}{2}\sum(p_\alpha^2 + \omega_\alpha^2 q_\alpha^2),$$

$$H_2 = \frac{1}{2}\sum(p_\alpha^2 + \omega_\alpha^2(q_\alpha^2 - q_{\alpha 0}^2)) + \Delta G$$

are the vibrational Hamiltonians in the excited and ground electronic states. $\widetilde{V}(t) = V(t) + \Delta$; Δ is the

electronic coupling matrix element, which induces transitions between the diabatic states.

$$V(t) = -\langle 1|\vec{d}\vec{E}(t)|2\rangle,$$

$\vec{d}$ is the transition dipole moment of the charge transfer electronic transition, $\vec{E}(t)$ is the electric pump field, $|2\rangle$ and $|1\rangle$ are the initial ground and excited states, respectively. The optical coupling operator is expressed as

$$V(t) = V_0 \exp(-\mathrm{i}\omega_e t - t^2/\tau_e^2),$$

where ω_e is the excitation pulse carrier frequency and τ_e its duration. For the sake of simplicity, we invoke the Condon approximation stating that both the optical coupling operator $V(t)$ and the electron exchange coupling Δ do not depend on the nuclear coordinates and momenta. ΔG is the free energy for CR and $E_r = \sum A_\alpha^2/2\omega_\alpha$ is the reorganization energy, $A_\alpha = \omega_\alpha^2 q_{\alpha 0}$, $q_\alpha, p_\alpha, \omega_\alpha$ and A_α being the mass-weighted coordinate, the momentum, the frequency and the electron-vibration coupling constant for the αth mode, respectively. We use the system of units where $\hbar = 1$.

The temporal evolution of the system is described by the quantum Liouville equation for the density operator ϱ

$$\mathrm{i}\frac{\partial \varrho}{\partial t} = [H, \varrho]. \tag{2}$$

The system is assumed to be initially at thermal equilibrium in the ground electronic state and its density matrix elements in the diabatic basis are $\varrho_{ij}(t \to -\infty) \to 0$, where $i, j = 1, 2$, with the exception of $\varrho_{22}(t \to -\infty) \to \varrho_{22}^{\mathrm{eq}} = \exp(-\beta H_2)/Tr\exp(-\beta H_2)$, with $\beta = 1/k_B T$, k_B and T being the Boltzmann constant and the temperature, respectively.

Using these initial conditions and applying the standard methods of time-dependent perturbation theory (see for example [27]) we obtain in first non-vanishing order for the change of the ground state $|2\rangle$ population due to the backward transition

$$\begin{aligned} W_2(t) = \Delta^2 \int_{-\infty}^{t} \mathrm{d}t_1 \int_{-\infty}^{t_1} \mathrm{d}t_2 \int_{-\infty}^{t_2} \mathrm{d}t_3 \int_{-\infty}^{t_3} \mathrm{d}t_4 V(t_3) \\ \times V^*(t_4)[G(t_1,t_2;t_3,t_4) + G(t_2,t_1;t_3,t_4) \\ + G(t_1,t_2;t_4,t_3) + G(t_2,t_1;t_4,t_3)], \end{aligned} \tag{3}$$

where

$$\begin{aligned} G(t_1,t_2;t_3,t_4) = \exp\{&-\mathrm{i}(t_1-t_2)\Delta G \\ &-\mathrm{i}(t_3-t_4)\Delta G + \mathrm{i}\Phi(t_1,t_2,t_3,t_4) \\ &- F(t_1,t_2,t_3,t_4)\}, \end{aligned} \tag{4}$$

$$\begin{aligned} \Phi(t_1,t_2,t_3,t_4) = \sum \frac{A_\alpha^2}{2\omega_\alpha^3}[&-\sin\omega_\alpha(t_1-t_2) \\ &+ \sin\omega_\alpha(t_1-t_3) + \sin\omega_\alpha(t_1-t_4) \\ &- \sin\omega_\alpha(t_2-t_3) - \sin\omega_\alpha(t_2-t_4) \\ &+ \sin\omega_\alpha(t_3-t_4)], \end{aligned}$$

$$\begin{aligned} F(t_1,t_2,t_3,t_4) = \sum \frac{A_\alpha^2}{2\omega_\alpha^3} \coth\frac{\beta\omega_\alpha}{2} \\ \times [2 - \cos\omega_\alpha(t_1-t_2) \\ + \cos\omega_\alpha(t_1-t_3) - \cos\omega_\alpha(t_1-t_4) \\ - \cos\omega_\alpha(t_2-t_3) + \cos\omega_\alpha(t_2-t_4) \\ - \cos\omega_\alpha(t_3-t_4)]. \end{aligned}$$

Eq. (3) constitutes the general solution of the problem in the non-adiabatic limit for an arbitrary vibrational spectrum. It takes into account a possible overlap between excitation and charge recombination.

In this equation, the forward transition to the excited state is only induced by the optical pulse $V(t)$ and the backward transition by the time-independent electronic coupling Δ. The rate of the backward non-radiative transition is equal to

$$k_2(t) = \frac{\mathrm{d}W_2(t)}{\mathrm{d}t}.$$

Furthermore, we define the spectral distribution of the coupling

$$J(\omega) = \frac{\pi}{2}\sum \frac{A_\alpha^2}{\omega_\alpha}\delta(\omega - \omega_\alpha).$$

This leads to the possibility of the substitution

$$\sum \frac{A_\alpha^2}{\omega_\alpha} f(\omega_\alpha) = \frac{2}{\pi}\int_0^\infty J(\omega) f(\omega)\,\mathrm{d}\omega,$$

where $f(\omega)$ is an arbitrary function. Now one can see that in electron transfer dynamics, the nuclear subsystem becomes apparent only through $J(\omega)$.

2.1. Model involving classical nuclear modes

This model is justified for systems without reorganization of high-frequency modes only. Its main advantage is its simplicity, hence the mechanism of the spectral effect is especially transparent.

To estimate the rate $k_2(t)$, we assume the short pulse limit $\tau_e\omega_\alpha \ll 1$ for all nuclear modes. This allows the sines and cosines in Eq. (4) to be expanded in powers of t_3 and t_4. Furthermore, the reorganization energy E_r is fairly large in polar solvents so that the inequality $\tau_b^2\omega_\alpha^2 \ll 1$, where $\tau_b^{-2} = 2E_r k_B T$, holds. In this case, the functions F and Φ can be expanded in series by $t_1 - t_2$ up to second order. Adopting the high-temperature limit ($\coth \beta\omega_\alpha/2 \simeq 2/\beta\omega_\alpha$), we obtain

$$F(t_1,t_2,t_3,t_4) \simeq E_r k_B T[(t_1-t_2)^2 + (t_3-t_4)^2 - 2X(t_1)(t_1-t_2)(t_3-t_4)], \quad (5)$$

$$\Phi(t_1,t_2,t_3,t_4) \simeq -E_r(1-2X(t_1))(t_1-t_2) + E_r(t_3-t_4), \quad (6)$$

where

$$X(t) = \frac{1}{\pi E_r}\int_0^\infty \frac{J(\omega)}{\omega}\cos\omega t\,\mathrm{d}\omega. \quad (7)$$

For $t > \tau_e, \tau_b$, the upper limit ($t_2 \to \infty$) in the integral Eq. (3) can be replaced because of the fast decay of the functions. Obviously, such a replacement overestimates the CR rate during the excitation pulse. The applicability of such an approximation requires the CR probability during the excitation pulse to be small, that is $k_{20}(t)\tau_e \ll 1$ for $t \leqslant \tau_e$. This condition is invariably fulfilled when the wave-packet is initially located away from the term crossing area.

The integral can now be calculated. The rate is

$$k_2(t) = W_e k_{20}(t), \quad (8)$$

where

$$W_e = \frac{\pi V_0^2 \tau_e}{\sigma_0}\exp\left[-\frac{(\delta\omega_e)^2}{2\sigma_0^2}\right], \quad (9)$$

$$k_{20}(t) = \Delta^2\frac{\sqrt{2\pi}}{\sigma(t)}\exp\left\{-\frac{[Q^* - Q(t)]^2}{2\sigma^2(t)}\right\}, \quad (10)$$

and with $Q^* = \Delta G + E_r$, $Q(t) = 2E_r(1 + k_B T\delta\omega_e/\sigma_0^2)X(t)$, $\sigma_0^2 = 2E_r k_B T + \tau_e^{-2}$, $\delta\omega_e = \Delta G + \omega_e - E_r$, and $\sigma^2(t) = 2E_r k_B T(1 - 2E_r k_B T X^2(t)/\sigma_0^2)$ which is the time-dependent dispersion of the wave-packet. W_e is the probability of excitation of the donor–acceptor complex, so that $k_{20}(t)$ is the time-dependent 'rate constant'.

When the inequality $2E_r k_B T \gg \tau_e^{-2}$ is fulfilled, the dispersion increases from $\sigma^2(0) \simeq \tau_e^{-2}$ at time zero to $\sigma^2(t \to \infty) = 2E_r k_B T$, because $X(t)$ decays from 1 to 0. In the opposite limit, the dispersion is almost time independent and $\sigma^2(t) \simeq 2E_r k_B T$. It should be emphasized that the dependence of the rate on the excitation frequency ω_e is also smaller when the spectral width of the excitation pulse, τ_e^{-1}, is large and in the limit $2E_r k_B T \ll \tau_e^{-2}$ one obtains $Q(t) \simeq 2E_r X(t)$ independently on the excitation frequency. This is the case that has been considered in papers [23,26].

The physics underlying Eq. (10) is rather transparent. It is well known that in the framework of the perturbation theory accepted here, the ET rate is proportional to the excited state population density in the vicinity of the term crossing area. Immediately after excitation, a Gaussian wave-packet is formed on the excited surface. The time dependence of the rate $k_{20}(t)$ reflects the propagation of the nuclear wave-packet on the excited potential energy surface. To show this, it is helpful to introduce the reaction coordinate (the collective electronic gap coordinate) $Q = \sum A_\alpha q_\alpha$. In terms of the reaction coordinate, the free energy surfaces are

$$U_1 = \frac{Q^2}{4E_r}, \quad U_2 = \frac{(Q-2E_r)^2}{4E_r} + \Delta G.$$

The term crossing point, $Q = Q^*$, is then determined with the condition $U_1 = U_2$. $Q(t)$ is the coordinate of the wave-packet maximum at time t. Its initial value $Q(0)$ can be found as follows: the initial shape of the wave-packet on the excited surface $f(Q)$ is determined by the product of the initial nuclear distribution in the ground state and the excitation pulse spectrum, that is

$$f(Q) \sim \exp\left(-\frac{U_2(Q)}{k_B T}\right) \times \exp\left(-\frac{(U_1 - U_2 - \omega_e)^2}{2\tau_e^{-2}}\right) \sim \exp\left(-\frac{(Q - Q(0))^2}{2\sigma^2(0)}\right). \quad (11)$$

This wave-packet shape immediately leads to the initial value of the rate $k_{20}(0) \sim f(Q^*)$ (Eq. (10)).

Basically, Eq. (10) differs from the non-equilibrium golden rule formula [22] in the explicit dependence of both the position and the width of the initial wave-packet on the excitation pulse characteristics. This implies that the comprehensive discussion of the applicability of the non-equilibrium golden rule given in article [22] has a direct bearing on Eq. (10). In particular, the replacement [22]

$$W_2(t) = W_e - \left[1 - \int_0^t dt' k_{20}(t') + \ldots\right] W_e \cong \left[1 - \exp\left[-\int_0^t dt' k_{20}(t')\right]\right] W_e, \quad (12)$$

is further used. It should be noticed that in the numerical calculations presented in the next section, the wave-packet propagation involves the motion through the term crossing surface and we impose the restriction that the ET probability at this stage has to be small.

2.2. Hybrid model

Ultrafast ET especially in the inverted regime, i.e., when $-\Delta G > E_r$, are usually described in terms of the hybrid model [20]. This model minimally includes a low-frequency solvent mode, a classical intramolecular low-frequency mode and quantum intramolecular high-frequency mode. A brief discussion of the nature of these modes is presented in the review [28]. We consider here the influence of the excitation pulse frequency on CR in the framework of the hybrid model. The assumptions commonly used include: (i) the time-scale of the intramolecular modes relaxation is shorter than that of CR; (ii) the spectral width of the high-frequency mode is negligibly small.

From Eq. (3) we obtain

$$k_{20}(t) = \frac{\Delta^2}{P}\frac{\sqrt{2\pi}}{\sigma_h(t)}\sum P_n \frac{\exp(-S)S^m}{m!} \times \exp\left\{-\frac{[Q_m^* - Q_n(t)]^2}{2\sigma_h^2(t)}\right\}, \quad (13)$$

where

$$P_n = \frac{\pi V_0^2 \tau_e}{(2E_r k_B T)^{1/2}}\frac{\exp(-S)S^n}{n!}\exp\left[-\frac{(\delta\omega_{en})^2}{4E_r k_B T}\right],$$

is the probability of optical transition to the state with high-frequency vibrational quantum number n, $Q_m^* = \Delta G + m\Omega + E_r$, $Q_n(t) = (\delta\omega_{en} + 2E_r)(E_{rm}/E_r)X(t)$, $\sigma_h^2(t) = 2k_B T(E_{rlf} + E_{rm}(1 - (E_{rm}/E_r)X^2 \times (t)))$, $P = \sum P_n$, $\delta\omega_{en} = \Delta G - n\Omega + \omega_e - E_r$, $S = E_{rhf}/\Omega$, Ω and E_{rhf} are the frequency and reorganization energy of the high-frequency mode, E_{rlf} and E_{rm} are reorganization energies of the low-frequency mode and of the medium, respectively, $E_r = E_{rlf} + E_{rm}$, $X(t) = x_1 \exp(-(t/\tau_1)^2) + \sum x_i \times \exp(-t/\tau_i)$ is the solvation coordinate, $x_i = E_{ri}/E_{rm}$ are the relative amplitudes of the contribution of the medium modes with relaxation times τ_i, the index 1 standing for the inertial solvation mode [29,30], $x_1 + \sum x_i = 1$. The conditions $2E_{rlf}k_B T \gg \tau_e^{-2}$, $\Omega\tau_e \gg 1$ and $\Omega\beta/2 \gg 1$ are assumed to be fulfilled. It should be noticed that the hybrid model is generalized to include the effects of non-Markovian solvent dynamics [30].

The physical meaning of Q_m^* and $Q_n(t)$ is very similar to that of Q^* and $Q(t)$ discussed in Section 2.1. The main difference is in their dependence on m or n, the number of excited high-frequency quanta.

Let us compare Eq. (13) and the standard hybrid model result [20]. To do this, one has to keep only in the sum over n of Eq. (13) the term with $\delta\omega_{en} = 0$, which corresponds to the vertical transition from the minimum of the ground state potential. The result of the standard hybrid model is then recovered if one put $\sigma_h^2(t) = 2E_{rlf}k_B T$. Indeed, in the standard hybrid model, the wave-packet projection on the solvation coordinate is supposed to be infinitely narrow and not to spread out with time.

3. Numerical calculations

Both Eqs. (10) and (13) predict a time-dependent CR rate constant and hence a non-exponential decay of the excited state population. To estimate quantitatively the effect of the pulse frequency on the CR dynamics, it is useful to introduce the following time-independent effective rate constant

$$k_{\mathrm{eff}}^{-1} = \int_0^{t_0} \exp\left[- \int_0^{t_1} k_{20}(t_2)\,\mathrm{d}t_2 \right] \mathrm{d}t_1, \qquad (14)$$

where t_1 is the time interval of the measurement of the excited state population in a typical experiment. Furthermore, t_0 is defined as the time after which the initial excited state population has decreased by a factor 100.

The theory of perturbation in electronic coupling predicts a minor spectral effect in the case of a single mode model. However, there can be a significant effect when two or more coordinates are involved. To demonstrate this, we consider a model with two Debye modes having very different relaxation times. We use Eq. (10) with $X(t) = x_1 \exp(-t/\tau_1) + x_2 \exp(-t/\tau_2)$. The results of the calculations are presented in Fig. 2. They show that the rate k_{eff} can go up (positive spectral effect) or down (negative spectral effect) with increasing excitation frequency. It should be emphasized that for the single mode model only the negative spectral effect is expected.

To understand the dependence of the CR rate on the excitation frequency, let us consider the motion of the wave-packet on the excited energy surface. The equipotential lines of the excited and ground electronic state and the trajectories of the wave-packet maximum are depicted in Fig. 3. The term crossing lines are marked as *ab* for weakly exergonic CR and *cd* for more exergonic CR. The trajectory number 1 corresponds to the smallest, 2 – medium and 3 – highest frequency ω_e. Because of the large difference in relaxation time of the two modes, the system moves first along the fast coordinate and then along the slow one. One can see that, when the excitation frequency is small (trajectory 1), most of the wave-packet passes through the term crossing line while moving along the fast coordinate. This feature decreases with increasing

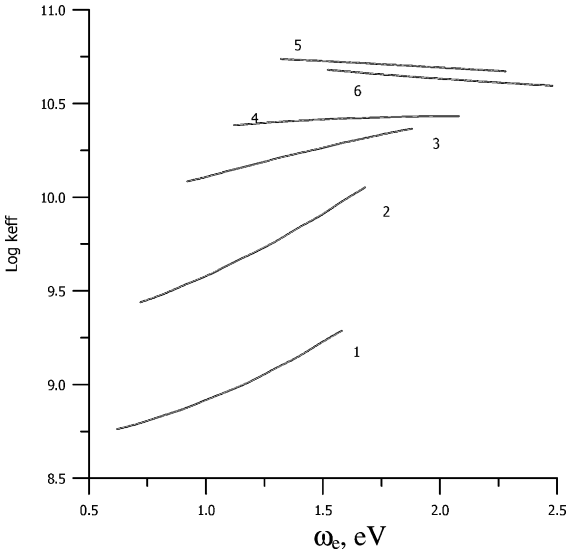

Fig. 2. Dependence of the logarithm of the effective electron transfer rate (in s^{-1}) on the carrier frequency for different values of Δ and ΔG. The parameters used here are: $T = 300$ K, $\tau_e = 50$ fs, $\tau_1 = 500$ fs, $\tau_2 = 10$ ps, $E_{r1} = 0.7$, $E_{r2} = 0.3$, (1) $\Delta = 0.007$, $\Delta G = -0.1$; (2) $\Delta = 0.006$, $\Delta G = -0.2$; (3) $\Delta = 0.0033$, $\Delta G = -0.4$; (4) $\Delta = 0.002$, $\Delta G = -0.6$; (5) $\Delta = 0.002$, $\Delta G = -0.8$; (6) $\Delta = 0.002$, $\Delta G = -1.0$. All energies are in eV.

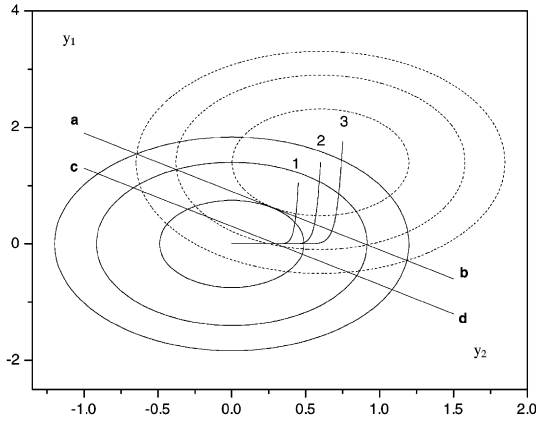

Fig. 3. Wave-packet trajectories on the excited free energy surface for a two Debye-like modes model. The dashed and solid lines are the equipotential curves of the ground and excited states, respectively. The term crossing lines are labeled as *ab* for $\Delta G = -0.1$ and *cd* for $\Delta G = -0.8$. The parameters used here are: $\tau_1 = 500$ fs, $\tau_2 = 10$ ps, $E_{r1} = 0.7$, $E_{r2} = 0.3$. All energies are in eV.

frequency (trajectories 2 and 3). Since the non-adiabatic ET probability is inversely proportional to the mean velocity of the wave-packet at the term crossing line, this leads to a positive spectral effect. Obviously, the positive spectral effect can be expected when the wave-packet maximum intersects the term crossing line while moving along the fast reaction coordinate. This is the case, in Fig. 3, for the weakly exergonic CR case (crossing line *ab*). A negative spectral effect can be expected if the wave-packet maximum intersects (or does not intersect at all, as it is in the inverted region) the term crossing line after relaxation of the fast mode. This case is illustrated in Fig. 3 for the more exergonic CR (crossing line *cd*). The more the wave-packet has to move on the slow coordinate before reaching the crossing line, the smaller the effective CR rate constant.

In the simulations presented here, the magnitude of Δ is varied while the CR free energy is changed. The reason for this is that the applicability of the perturbation theory in electronic coupling depends on ΔG and that large spectral effects are only expected when Δ is close to the upper limit of applicability.

Fig. 4 shows the dependence of the spectral effect on the electronic coupling Δ at various magnitudes of ΔG for the same model as in Fig. 2. In the region $0 < -\Delta G < E_{r1}$ (here E_{r1} is the reorganization energy of the fast mode), the spectral effect increases with increasing Δ, at least in the vicinity of zero. This dependence can be easily understood by considering that the fraction of population undergoing CR during relaxation increases with Δ. For each value of the CR free energy in the region $0 < -\Delta G < E_{r1}$, there is a distinct maximum of the spectral effect. This maximum approaches $\Delta = 0$ with increasing driving force and disappears when $-\Delta G > E_{r1}$. In the inverted region, only a descending curve is predicted, i.e., the spectral effect becomes more and more negative. Of course, the largest effect is often beyond the limit of applicability of the perturbation theory.

Fig. 5 shows the free energy dependence of the spectral effect according to the hybrid model for different sizes of the electronic coupling. For a given Δ value, the spectral effect has a pronounced

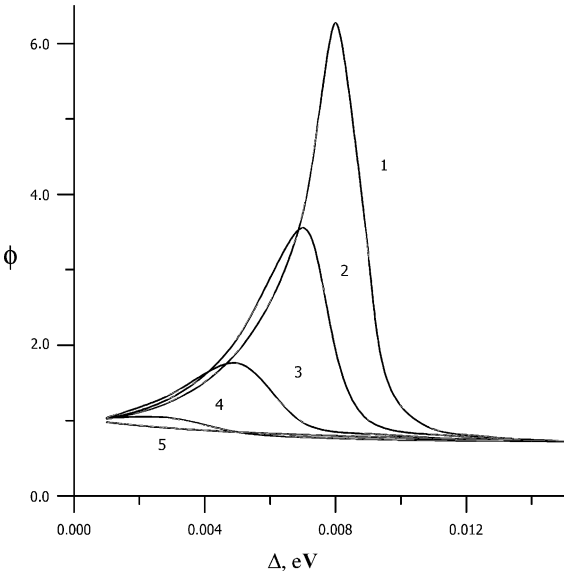

Fig. 4. Spectral effect $\phi = k_{\text{eff}}(\omega_{\max})/k_{\text{eff}}(\omega_{\min})$ as a function of electronic coupling Δ. The parameters used here are: $T = 300$ K, $\tau_e = 50$ fs, $\tau_1 = 500$ fs, $\tau_2 = 10$ ps, $E_{r1} = 0.7$, $E_{r2} = 0.3$, (1) $\Delta G = -0.25$; (2) $\Delta G = -0.3$; (3) $\Delta G = -0.4$; (4) $\Delta G = -0.6$; (5) $\Delta G = -1.2$. $\omega_{\min}$ and $\omega_{\max}$ are the excitation frequencies at half the absorption band maximum on the low- and high-frequency sides, respectively. All energies are in eV.

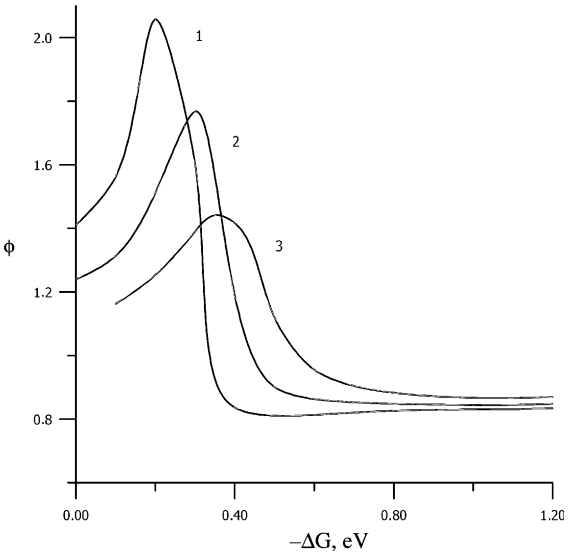

Fig. 5. Spectral effect ϕ according to the hybrid model as a function of CR free energy ΔG. The parameters used here are: $T = 300$ K, $\tau_e = 50$ fs, $\tau_1 = 1$ ps, $\tau_2 = 5$ ps, $\tau_3 = 30$ ps, $\Omega = 0.19$, $E_{\text{rlf}} = 0.2$, $E_{\text{rhf}} = 0.3$, $E_{\text{rm}} = 0.7$, $x_1 = 0.45$, $x_2 = 0.45$, $x_3 = 0.1$, (1) $\Delta = 0.01$; (2) $\Delta = 0.008$; (3) $\Delta = 0.006$. All energies are in eV.

maximum in the normal region ($-\Delta G < E_r$). In the inverted region, the effect is always negative. The mechanism of the spectral effect and its dependence on Δ and ΔG are qualitatively the same as that for two mode model.

4. Conclusion

The dependence of the effective CR rate on the carrier frequency of the excitation laser pulse is predicted to be sufficiently pronounced to be experimentally observable for ultrafast CR. This is in agreement with preliminary results [31]. The free energy dependence of the magnitude of the spectral effect is not monotonous. It first increases with increasing $-\Delta G$ and then goes down becoming negative for $-\Delta G > -\Delta G^*$. This critical value, $-\Delta G^*$, above which a negative spectral effect is predicted, depends on the magnitude of electronic coupling, the larger the coupling the smaller $-\Delta G^*$.

In the region where $-\Delta G < E_{rf}$, E_{rf} being the reorganization energy of all classical modes except the slowest one, both negative and positive spectral effects can be observed. Its magnitude increases first and then reduces with increasing coupling. At sufficiently strong coupling, the spectral effect becomes invariably negative. Although this limit is often far beyond the area of applicability of the perturbation theory, this prediction is qualitatively correct. In this case, the term crossing line in Fig. 3 can be seen as a completely absorbing line and thus the spectral effect is negative. With the theory presented here, no conclusion can of course be obtained for the strong coupling limit, i.e., when the adiabatic regime is realized. In the inverted region on the other hand, only the negative spectral effect is expected.

This analysis has shown the existence of two mechanisms resulting to spectral effects of opposite signs. The mechanism for positive spectral effect lies in the fact that with increasing pulse carrier frequency, the fraction of the wave-packet cutting the term crossing line while moving along the slow coordinate is larger. The negative spectral effect is due to the fact that with increasing ω_e, the wave-packet is initially located farther from the term crossing line. This results to a delayed launching of the ET reaction and, as a consequence, to a decrease of the effective rate. In reality, both mechanisms compete and both positive and negative effects can be observed.

In order to have a marked spectral effect, the electron coupling should not be too small. Indeed, the effect disappears in the limit of weak electron coupling. Nevertheless, the most interesting region for strong spectral effects is often beyond the limit of applicability of the perturbation theory and this is the main weakness of the approach adopted in this Letter. One way to circumvent this problem is to use the stochastic model for medium reorganization. We plan to do this in the immediate future.

Acknowledgements

This work was supported by Russian fund for basic research grants (02-03-32275 and 02-03-81008).

References

[1] T. Kobayashi, Y. Takagi, H. Kandori, K. Kemnitz, K. Yoshihara, Chem. Phys. Lett. 180 (1991) 416.
[2] E. Akesson, G.C. Walker, P.F. Barbara, J. Chem. Phys. 95 (1991) 4188.
[3] P.J. Reid, C. Silva, P.F. Barbara, L. Karki, J.T. Hupp, J. Phys. Chem. 99 (1995) 2609.
[4] Y. Nagasawa, A.P. Yartsev, K. Tominaga, P.B. Bisht, A.E. Johnson, K. Yoshihara, J. Phys. Chem. 99 (1995) 653.
[5] M. Seel, S. Engleitner, W. Zinth, Chem. Phys. Lett. 275 (1993) 363.
[6] M.E Michel-Beyerle, G.J. Small, R.M. Hochstrasser, G.L. Hofacker, Chem. Phys. 197 (1995) 223.
[7] K. Wynne, G.D. Reid, R.M. Hochstrasser, J. Chem. Phys. 105 (1996) 2287.
[8] I.V. Rubtsov, K. Yoshihara, J. Phys. Chem. A 101 (1997) 6138.
[9] B. Wolfseder, L. Seidner, W. Domcke, G. Stock, M. Seel, S. Engleitner, W. Zinth, Chem. Phys. 233 (1998) 323.
[10] S. Iwai, S. Murata, M. Tachiya, J. Chem. Phys. 109 (1998) 5963.
[11] Q.-H. Xu, G.D. Scholes, M. Yang, G.R. Fleming, J. Phys. Chem. A 103 (1999) 10348.
[12] E. Vauthey, J. Phys. Chem. A 105 (2001) 340.
[13] N.G. Bakshiev, Opt. Spectrosc. (USSR) 16 (1964) 446.
[14] V. Hizhnyakov, I.Yu. Tekhver, Phys. Status Solidi 21 (1967) 75.

[15] Yu.T. Mazurenko, N.G. Bakshiev, Opt. Spectrosc. (USSR) 28 (1970) 490.
[16] L.D. Zusman, A.B. Helman, Opt. Spectrosc. (USSR) 53 (1982) 248.
[17] B. Bagchi, D.W. Oxtoby, G.R. Fleming, Chem. Phys. 86 (1984) 25.
[18] G. Van der Zwan, J.T. Hynes, J. Phys. Chem. 89 (1985) 4181.
[19] R.F. Loring, Y.J. Yan, S. Mukamel, J. Chem. Phys. 87 (1987) 5840.
[20] G.C. Walker, E. Akesson, A.E. Johnson, N.E. Levinger, P.F. Barbara, J. Phys. Chem. 96 (1992) 3728.
[21] M. Tachiya, S. Murata, J. Am. Chem. Soc. 116 (1994) 2434.
[22] R.D. Coalson, D.G. Evans, A. Nitzan, J. Chem. Phys. 101 (1994) 436.
[23] M. Cho, R.J. Silbey, J. Chem. Phys. 103 (1995) 595.
[24] W. Domcke, G. Stock, Adv. Chem. Phys. 100 (1997) 1.
[25] J.M. Jean, J. Phys. Chem. A 102 (1998) 7549.
[26] A.I. Ivanov, V.V. Potovoi, Chem. Phys. 247 (1999) 245.
[27] S. Mukamel, Principles of Nonlinear Optical Spectroscopy, Oxford University Press, New York, 1995.
[28] B. Bagchi, N. Gayathri, Adv. Chem. Phys. 107 (1999) 1.
[29] K. Tominaga, D.A.V. Kliner, A.E. Johnson, N.E. Levinger, P.F. Barbara, J. Chem. Phys. 98 (1993) 1228.
[30] O. Nicolet, E. Vauthey, J. Phys. Chem. A 106 (2002) 5553.
[31] A. Morandeira, A. Furstenberg, O. Nicolet, S. Pages, B. Lang, E. Vauthey, Chimia 12 (2002) 690.